

Magnetohydrodynamic simulations of stellar differential rotation and meridional circulation

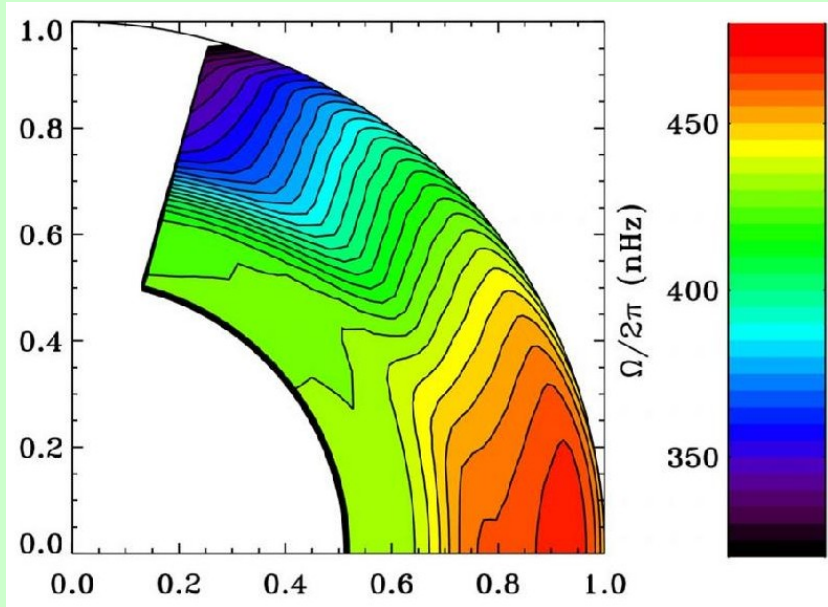
(submitted to A&A, arXiv:1407.0984)

Bidya Binay Karak

(Nordita fellow)

In collaboration with Petri J. Kaepyla, Maarit J. Kaepyla,
and Axel Brandenburg

Internal solar rotation from helioseismology



Gilman & Howe (2003)

=> **Solar-like** differential rotation observed in rapidly rotating dwarfs (e.g. Collier Cameron 2002)

When polar regions rotate faster than equator regions is called **anti-solar differential rotation**.

- observed in slowly rotating stars (e.g., K giant star HD 31993; Strassmeier et al. 2003; Weber et al. 2005).

Transition from solar-like to anti-solar differential rotation in simulations (Gilman 1978; Brun & Palacios 2009; Chan 2010; Kapyla et al. 2011; Guerrero et al. 2013; Gastine et al. 2014)

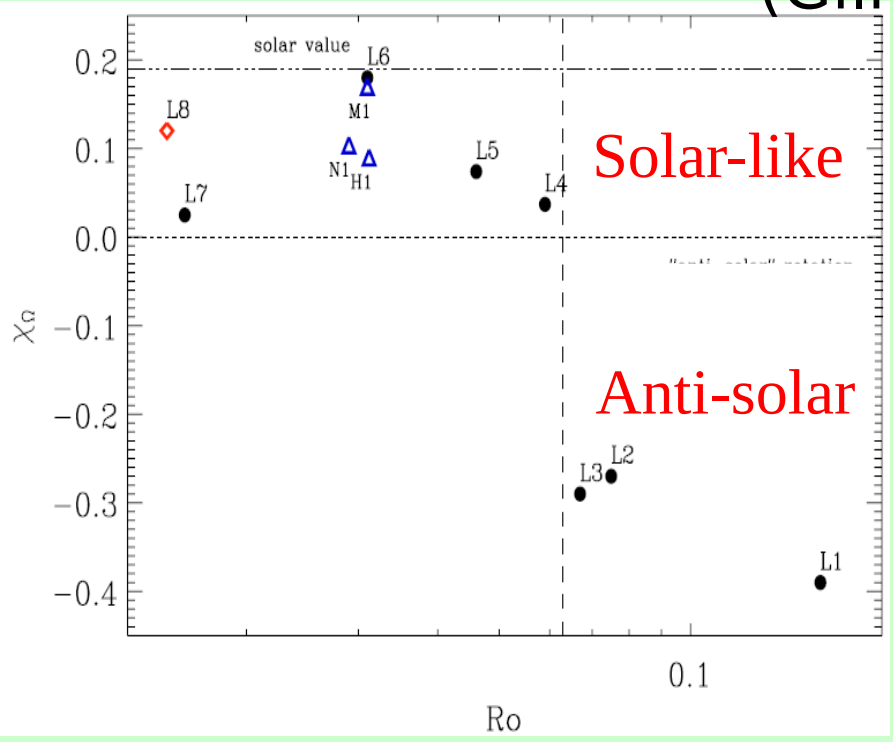
Independent of model setup.

$$Co = \frac{2\Omega_0}{u_{rms}k_f}$$

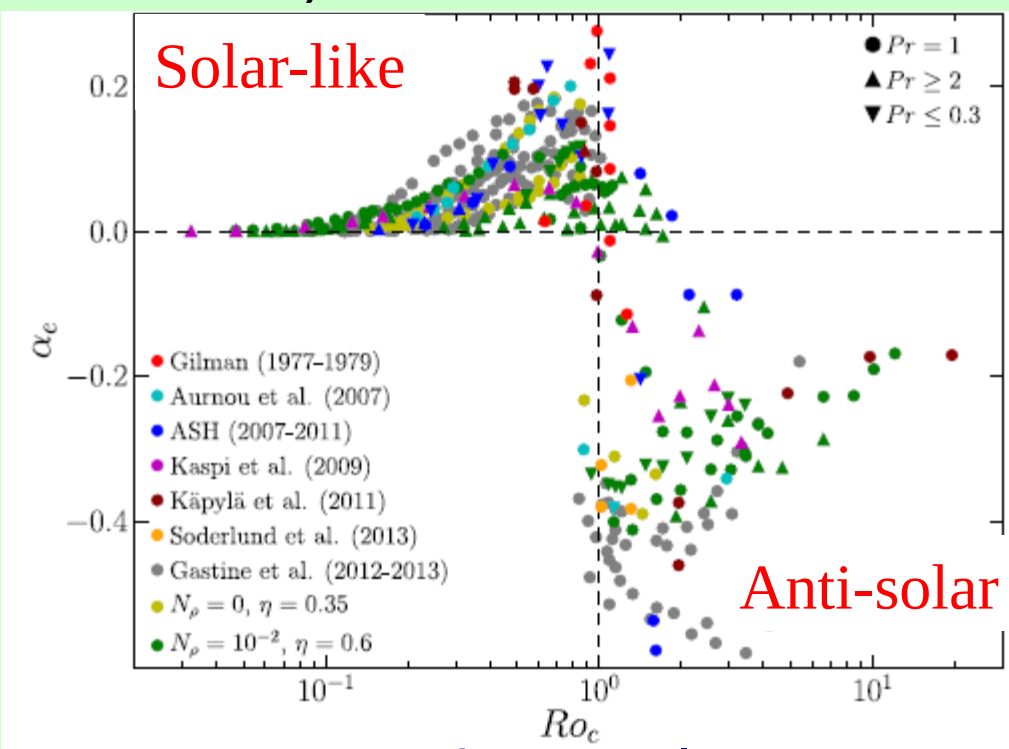
$$Ro_c = \left(\frac{Ra}{PrTa} \right)^{1/2}$$

(Gilman 1977)

$$Ta = (2\Omega_0 \Delta r^2 / \nu)^2$$

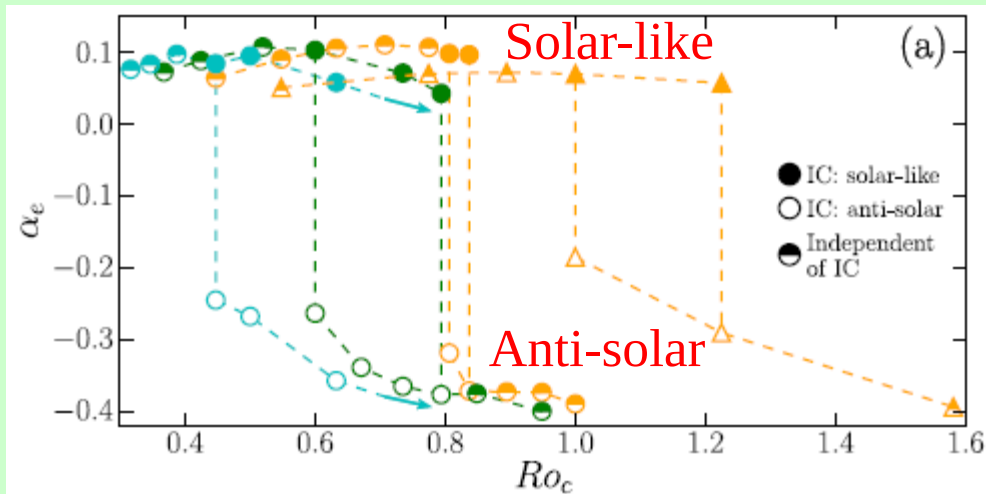


Guerrero et al. (2013)



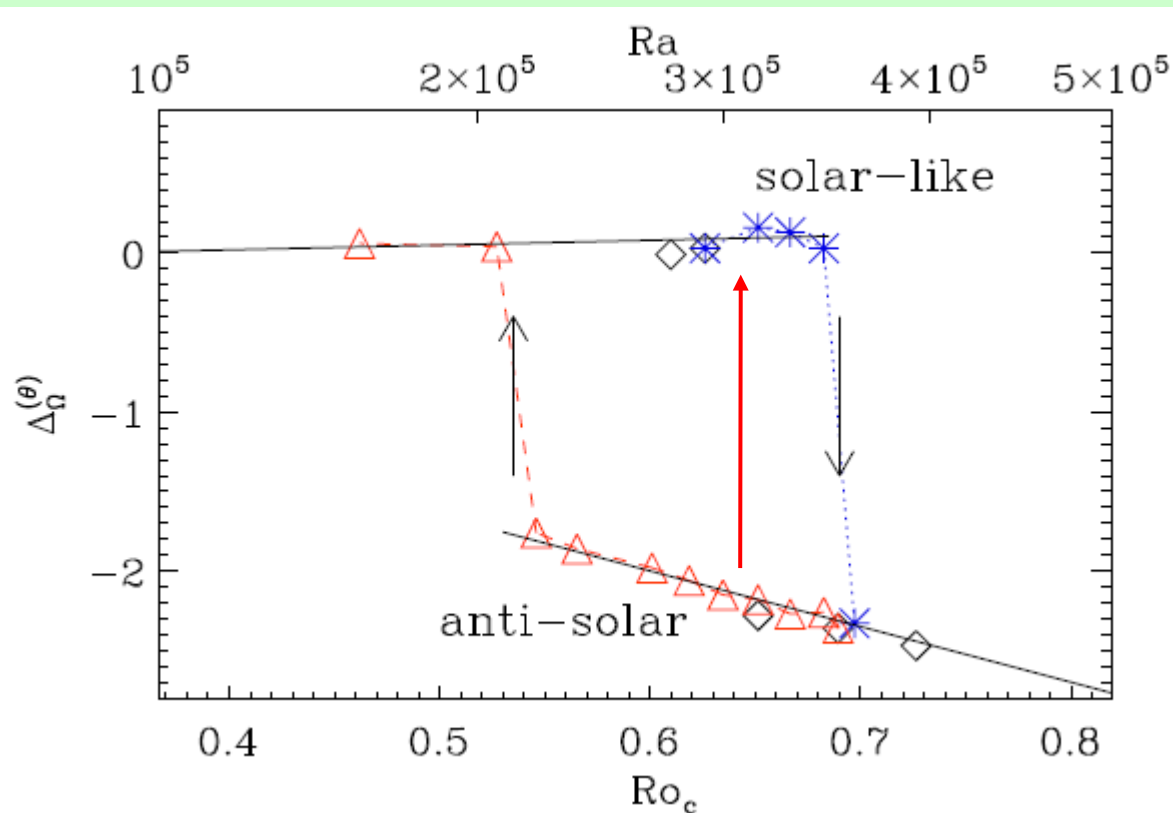
Gastine et al.

Bistability of differential rotation



Observed in many HD simulations

Gastine et al. (2014)
from Boussinesq convection.



Kapyla et al. (2014)
in fully compressible simulations

Model equations (also see Joern Warnecke's talk)

$$\frac{\partial \mathbf{A}}{\partial t} = \mathbf{u} \times \mathbf{B} - \mu_0 \eta \mathbf{J},$$

$$\frac{D \ln \rho}{Dt} = -\nabla \cdot \mathbf{u},$$

$$\frac{D \mathbf{u}}{Dt} = \mathbf{g} - 2\boldsymbol{\Omega}_0 \times \mathbf{u} + \frac{1}{\rho} (\mathbf{J} \times \mathbf{B} + \nabla \cdot 2\nu \rho \mathbf{S} - \nabla p)$$

$$T \frac{Ds}{Dt} = -\frac{1}{\rho} \nabla \cdot (\mathbf{F}^{\text{rad}} + \mathbf{F}^{\text{SGS}}) + 2\nu \mathbf{S}^2 + \frac{\eta \mu_0}{\rho} \mathbf{J}^2,$$

$$p = (\gamma - 1)\rho e, \quad e = c_V T$$

$$\mathbf{F}^{\text{rad}} = -K \nabla T \quad \text{and} \quad \mathbf{F}^{\text{SGS}} = -\chi_{\text{SGS}} \rho T \nabla s.$$

$$K(r) = K_0 [n(r) + 1]$$

$$n(r) = \delta n (r/r_0)^{-15} + n_{\text{ad}} - \delta n \quad n_{\text{ad}} = 1.5$$

$$K_0 = (\mathcal{L}/4\pi) c_V (\gamma - 1) (n_{\text{ad}} + 1) \rho_0 \sqrt{GM_\odot R_\odot}.$$

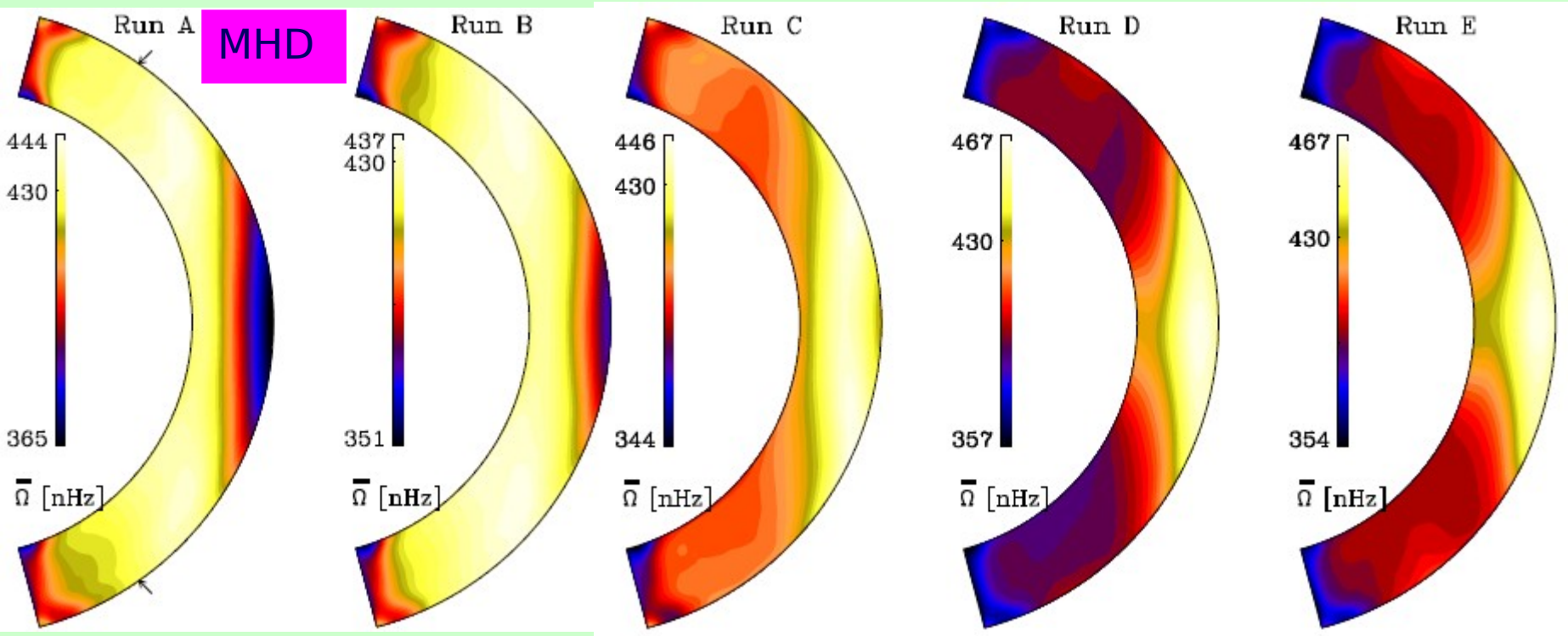
Computations are performed in spherical wedge geometry:

$$0.72R \leq r \leq 0.97R$$

$$15^\circ \leq \theta \leq 165^\circ$$

$$0 \leq \varphi \leq \frac{\pi}{2}$$

- **We performed several simulations by varying the rotational influence on the convection.**
- **We regulate the convective velocities by varying the amount of heat transported by thermal conduction, turbulent diffusion, and resolved convection.**

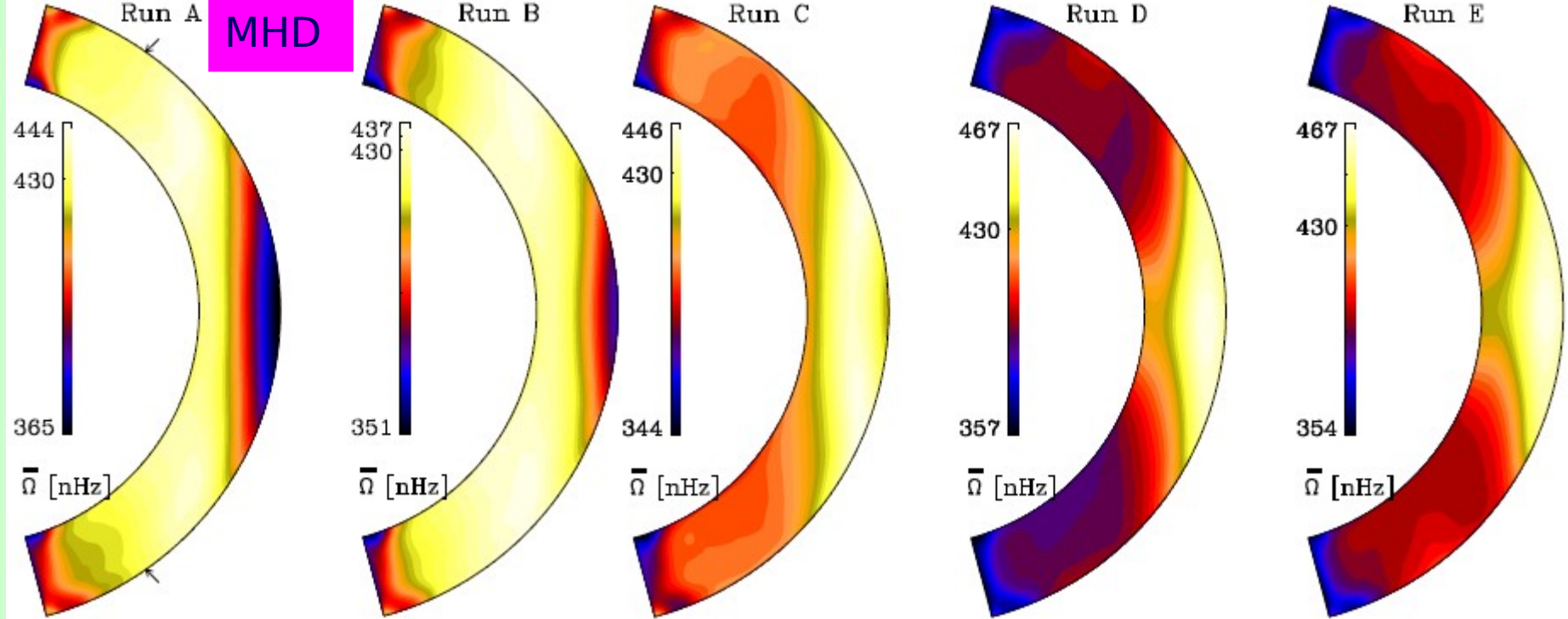


$Co = 1.34, 1.35, 1.44, 1.67, 1.75$

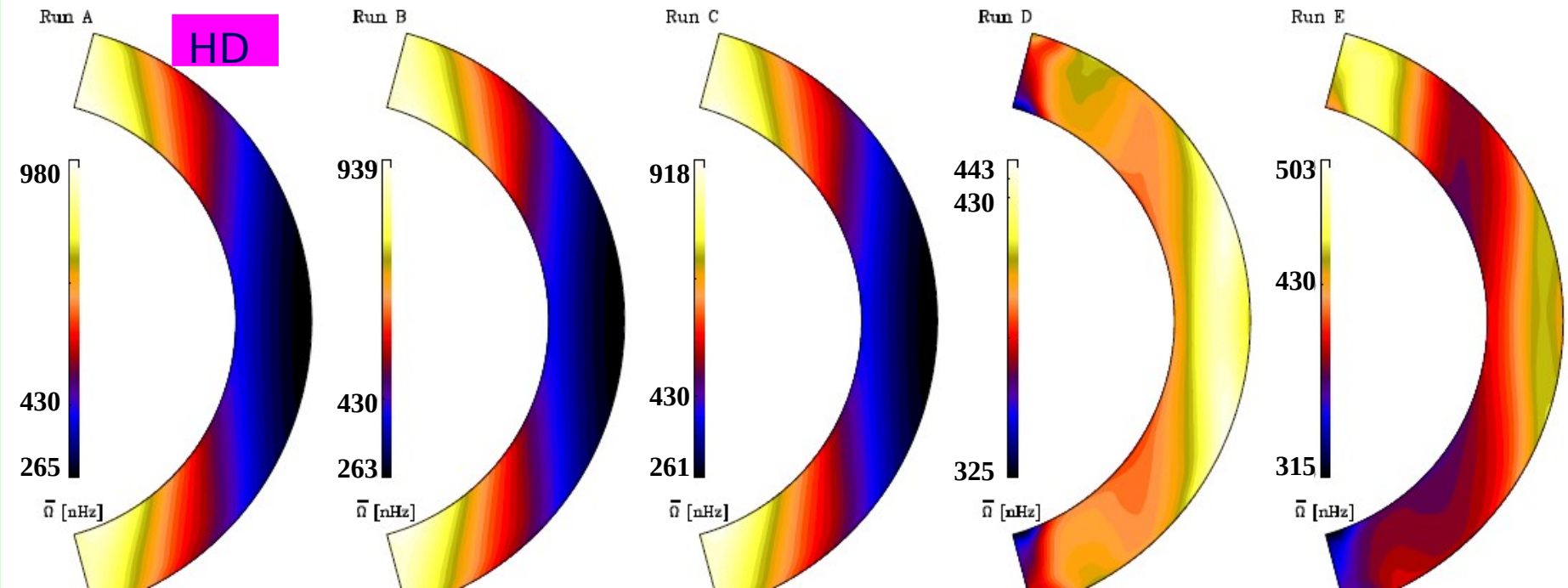


Rotational effect on the convection is increased

MHD

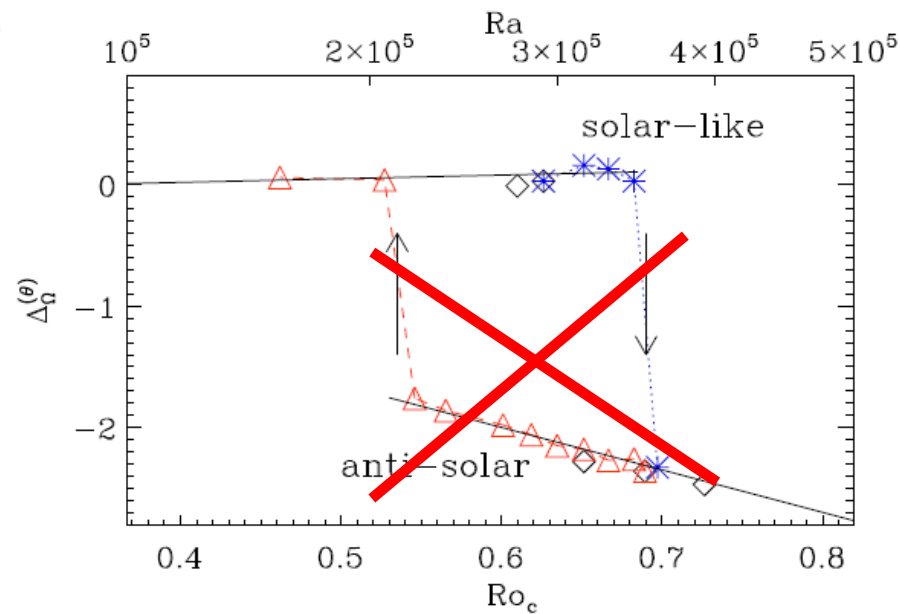
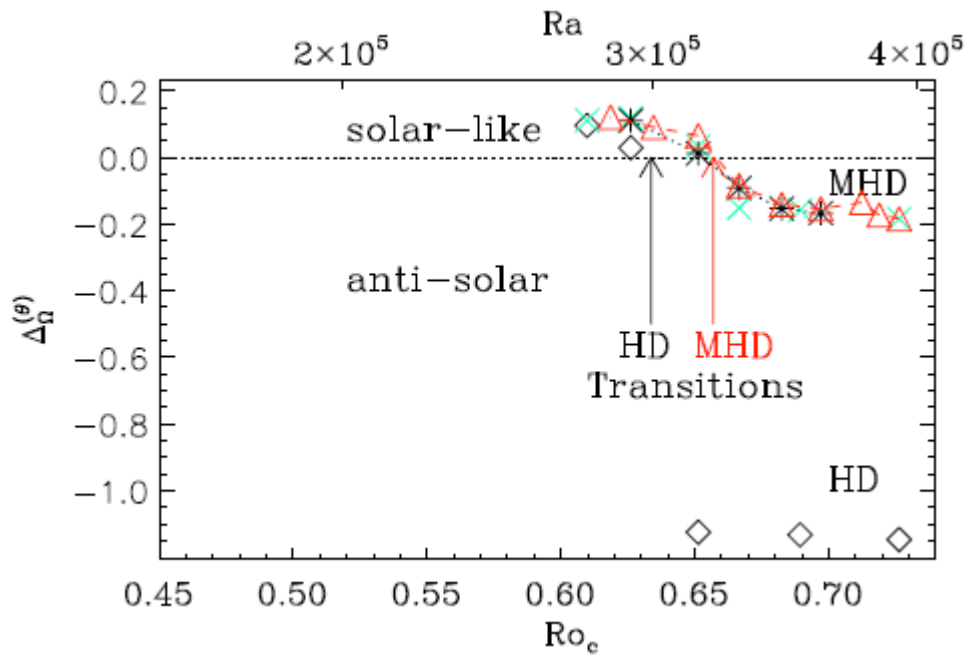


HD



Identifying the transition of differential rotation

$$\Delta_{\Omega}^{(\theta)} = \frac{\Omega_{\text{eq}} - \Omega_{55}}{\Omega_{\text{eq}}}$$



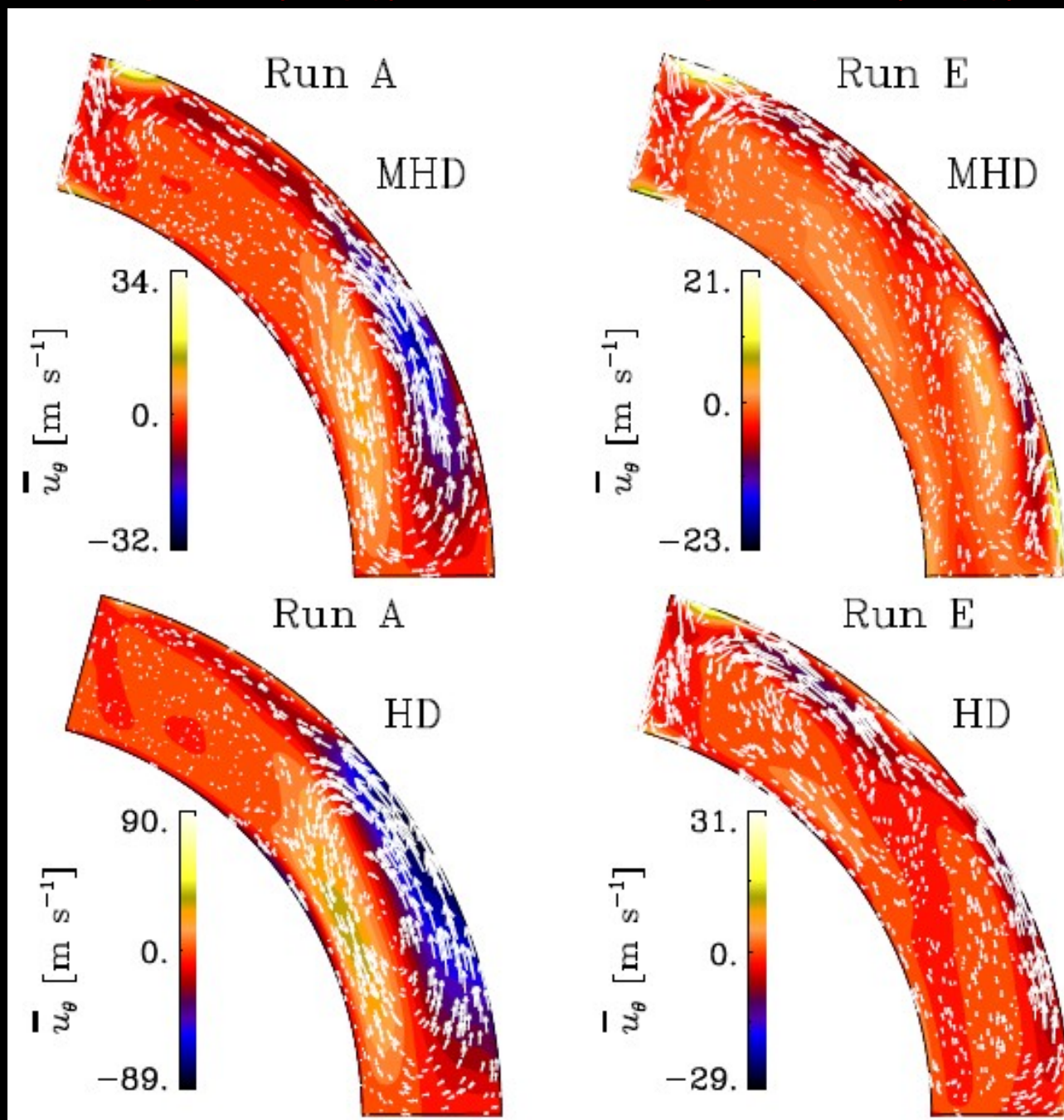
Magnetic field helps to produce more solar-like differential rotation

No evidence of *bistability!*
Gastine et al. (2014)
Kapyla et al. (2014)

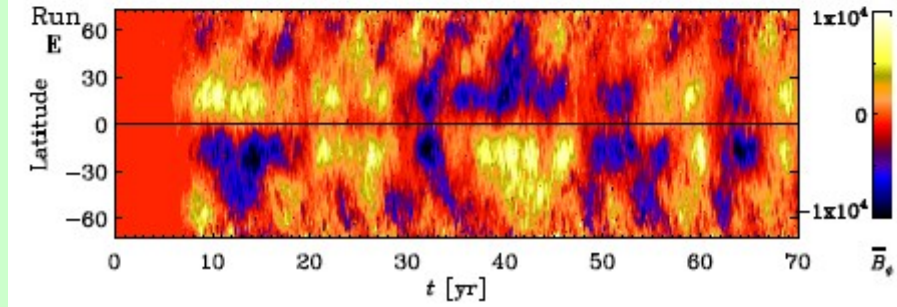
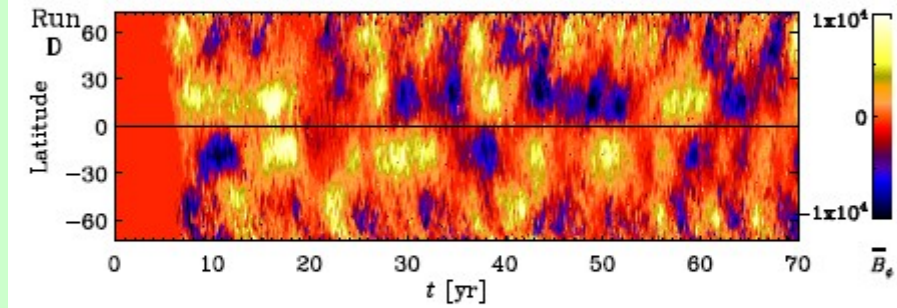
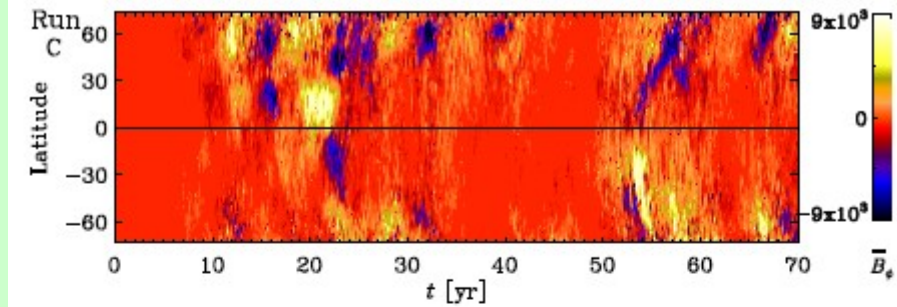
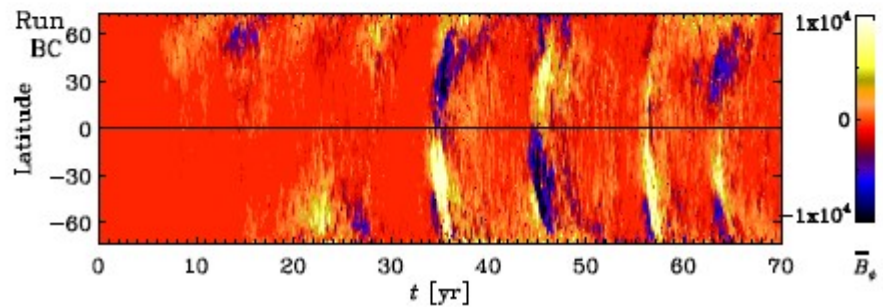
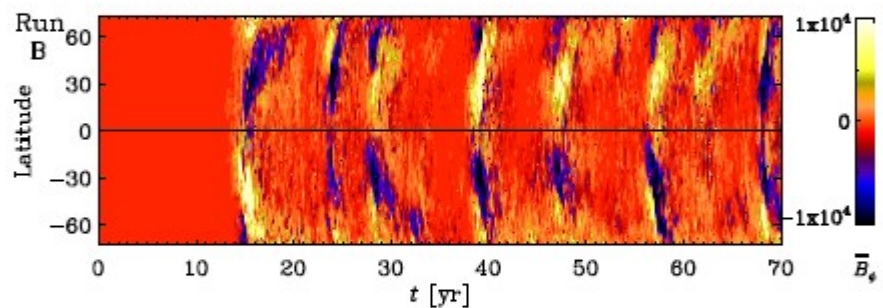
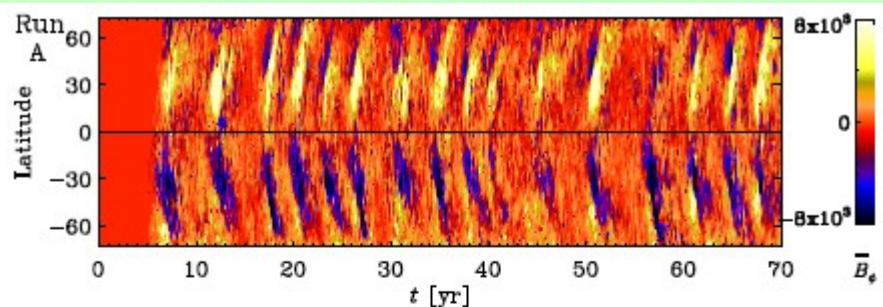
A-S diff. rot.

S-L diff. rot.

**Meridional
circulation**

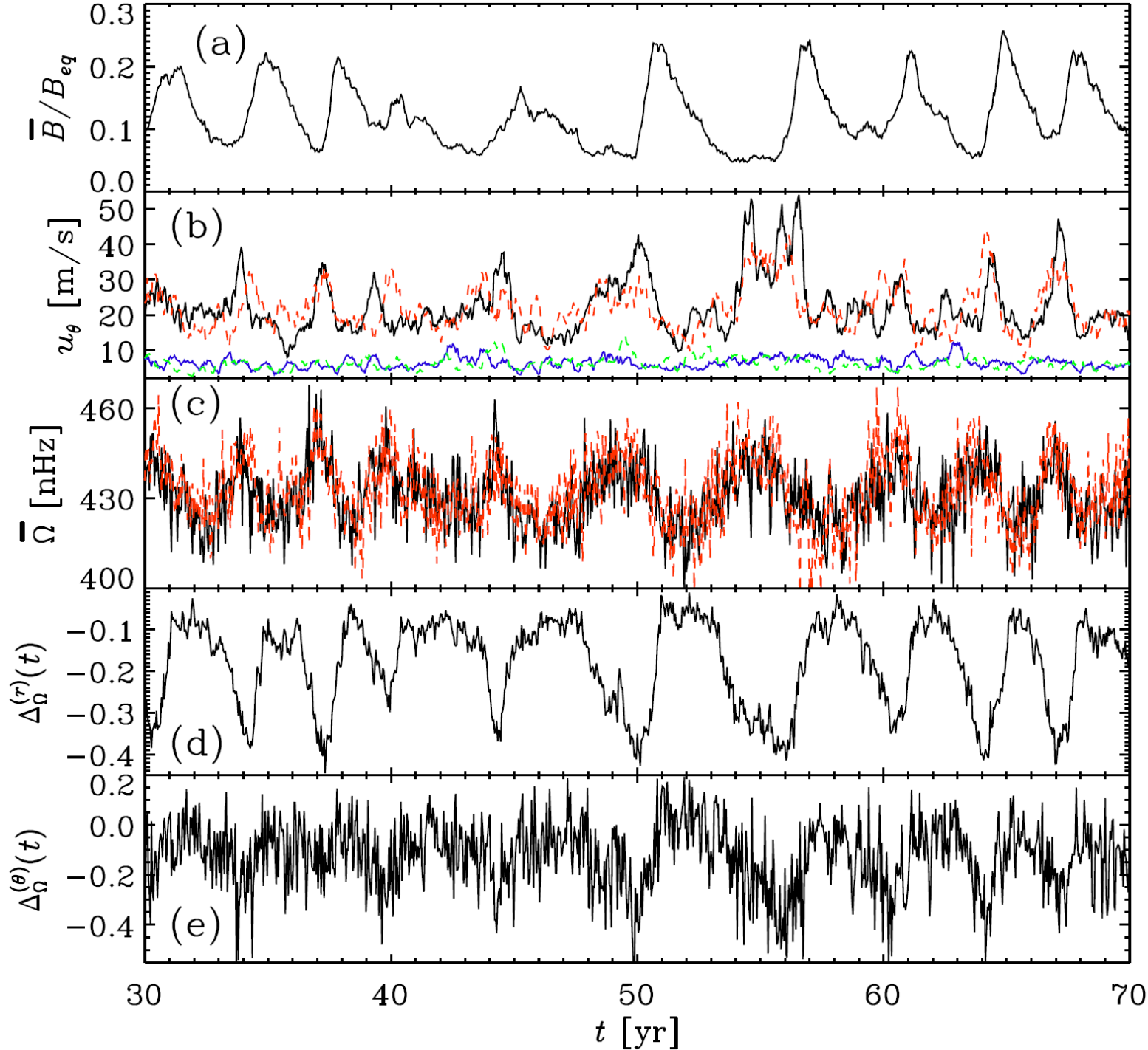


Azimuthally averaged **toroidal field** near the bottom of SCZ



Runs produce **anti-solar differential** rotation

Runs produce **solar-like differential** rotation



From
Run A
(AS
Diff.Rot)

Variation:
~ 50%

~ 6%

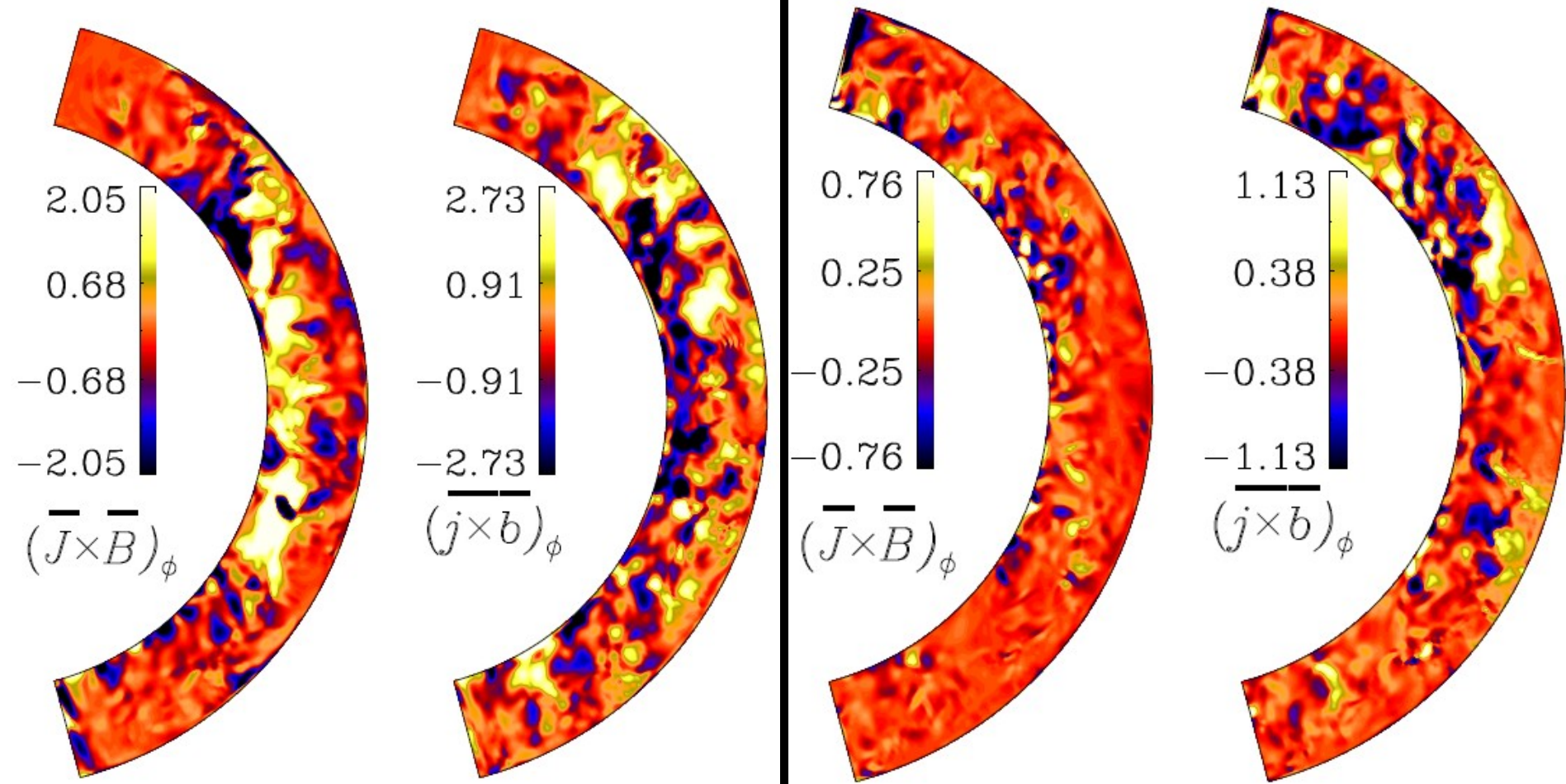
~ 75%

How does the variation in large-scale flow come?

Variation of Lorentz forces over magnetic cycle

Maximum

Minimum



Angular momentum fluxes (e.g., Brun et al. 2004; Beaudoin et al. 2013)

$$\frac{1}{r^2} \frac{\partial(r^2 \mathcal{F}_r)}{\partial r} + \frac{1}{r \sin \theta} \frac{\partial(\sin \theta \mathcal{F}_\theta)}{\partial \theta} = 0$$

$$\mathcal{F}_r = \bar{\rho} r \sin \theta \left[-\nu r \frac{\partial}{\partial r} \left(\frac{\hat{v}_\phi}{r} \right) + \widehat{v'_r v'_\phi} + \hat{v}_r (\hat{v}_\phi + \Omega r \sin \theta) \right]$$

Reynolds stress

$$\left[-\frac{1}{4\pi\bar{\rho}} \widehat{B'_r B'_\phi} - \frac{1}{4\pi\bar{\rho}} \hat{B}_r \hat{B}_\phi \right]$$

$$\mathcal{F}_\theta = \bar{\rho} r \sin \theta \left[-\nu \frac{\sin \theta}{r} \frac{\partial}{\partial \theta} \left(\frac{\hat{v}_\phi}{\sin \theta} \right) + \widehat{v'_\theta v'_\phi} + \hat{v}_\theta (\hat{v}_\phi + \Omega r \sin \theta) \right]$$

Maxwell stress

$$\left[-\frac{1}{4\pi\bar{\rho}} \widehat{B'_\theta B'_\phi} - \frac{1}{4\pi\bar{\rho}} \hat{B}_\theta \hat{B}_\phi \right]$$

$$Q_{r\phi} = \overline{u'_r u'_\phi} \equiv \Lambda_V \sin \theta \bar{\Omega} - \nu_t r \sin \theta \frac{\partial \bar{\Omega}}{\partial r}$$

$$Q_{\theta\phi} = \overline{u'_\theta u'_\phi} \equiv \Lambda_H \cos \theta \bar{\Omega} - \nu_t \sin \theta \frac{\partial \bar{\Omega}}{\partial \theta}$$

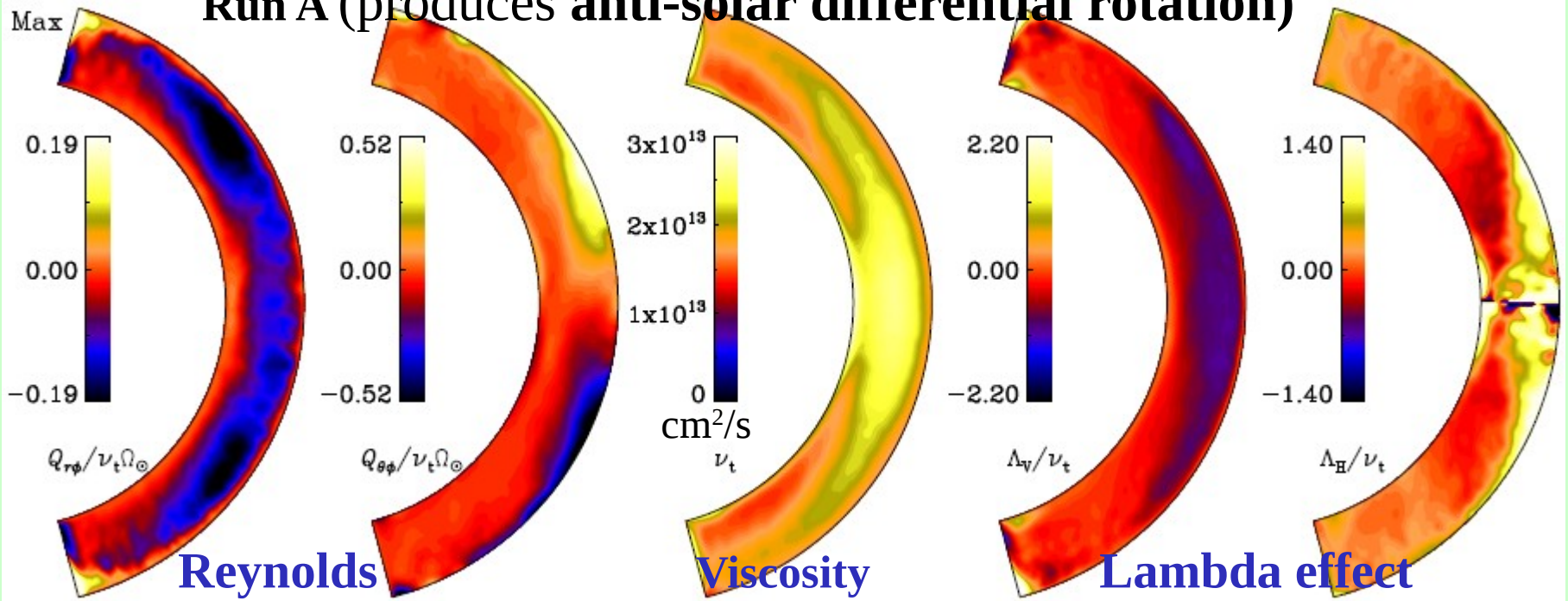
$$\nu_t = \frac{1}{3} u_{\text{rms}} \alpha_{\text{MLT}} H_p$$

(Rudiger 1980,1989)

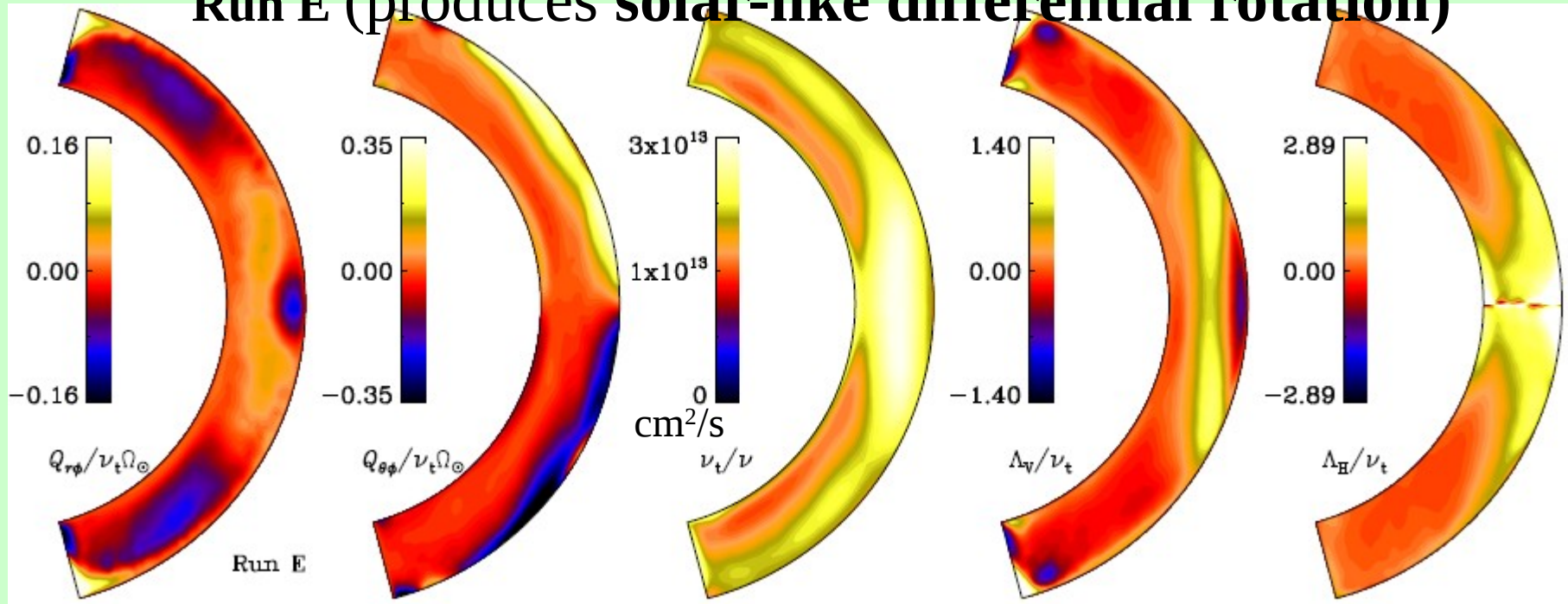
Mean
Tension

Coriolis force

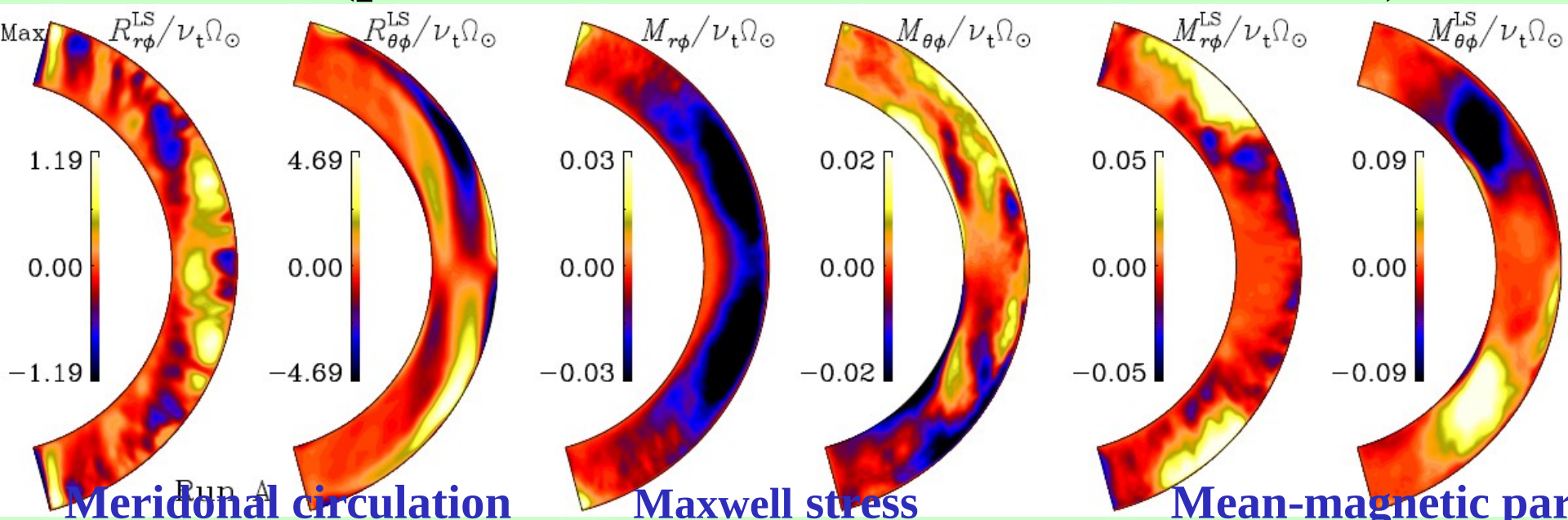
Run A (produces anti-solar differential rotation)



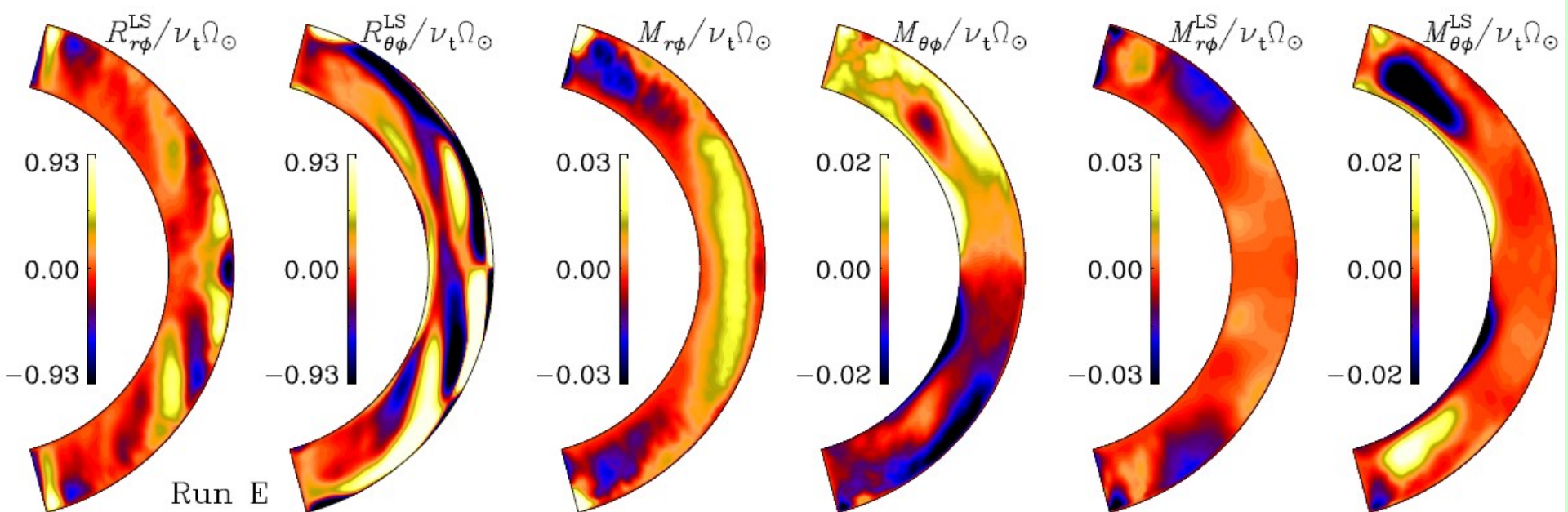
Run E (produces solar-like differential rotation)



Run A (produces anti-solar differential rotation)

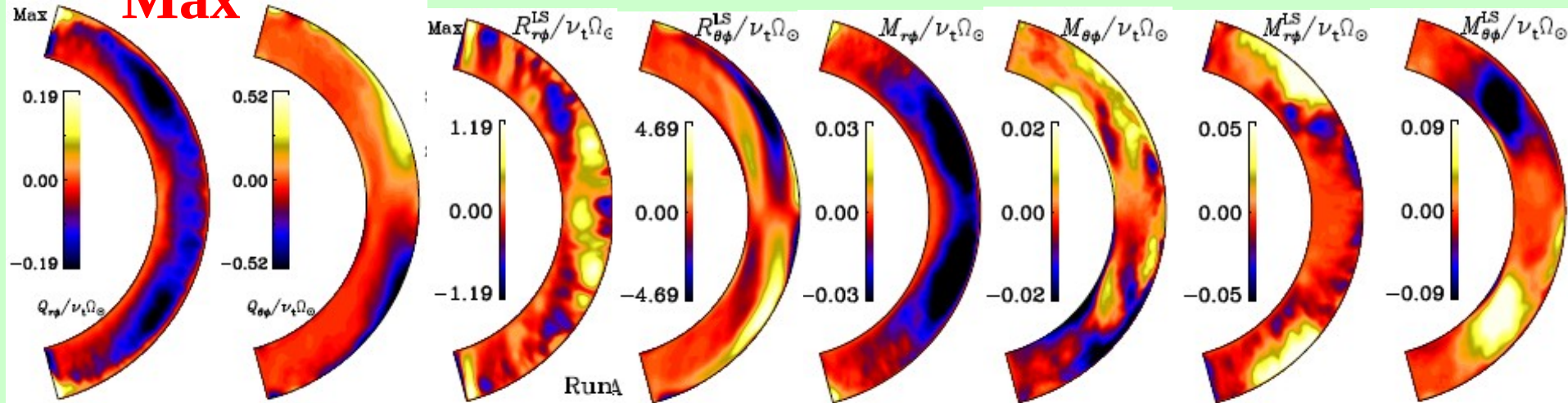


Run E (produces solar-like differential rotation)

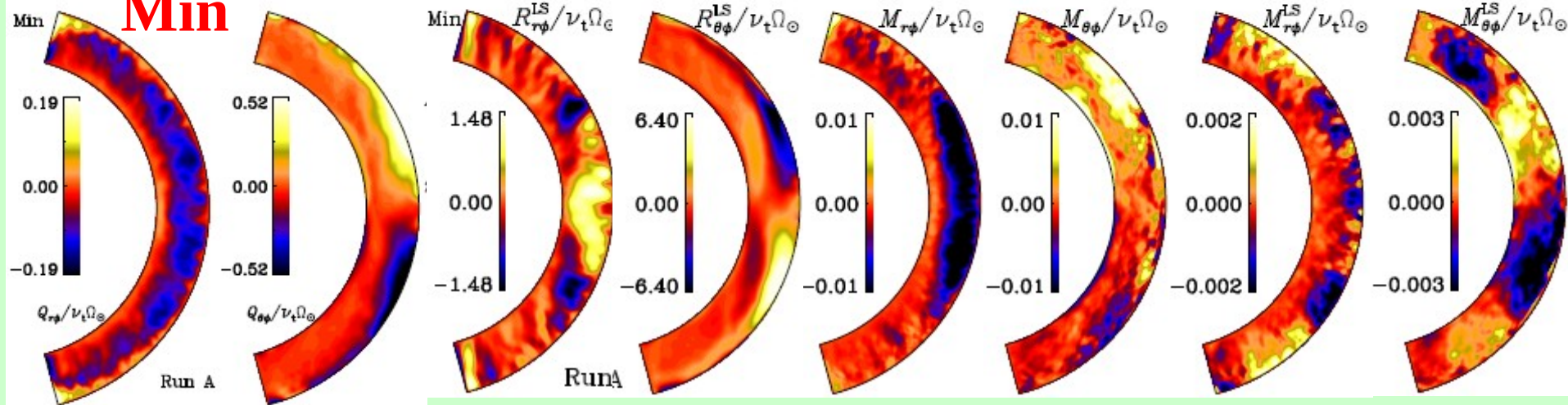


Temporal variation: From Run A (anti-solar diff. rot.)

Max



Min



Reynolds stress

Meridional
circulation

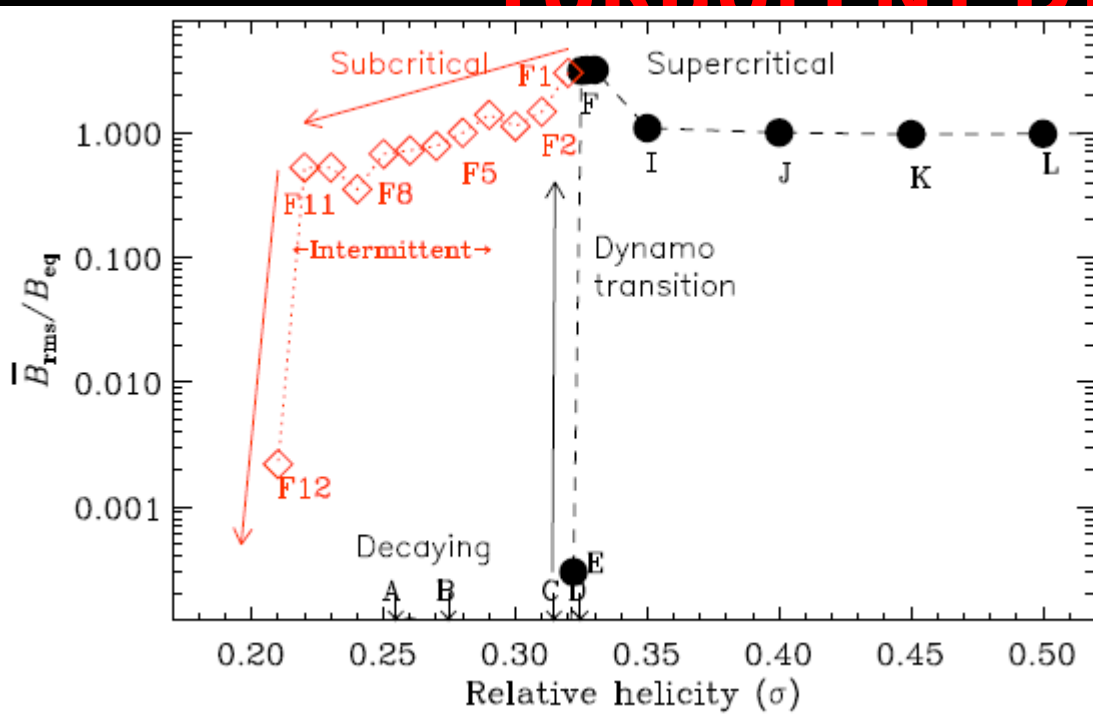
Maxwell stress

Mean-magnetic
part

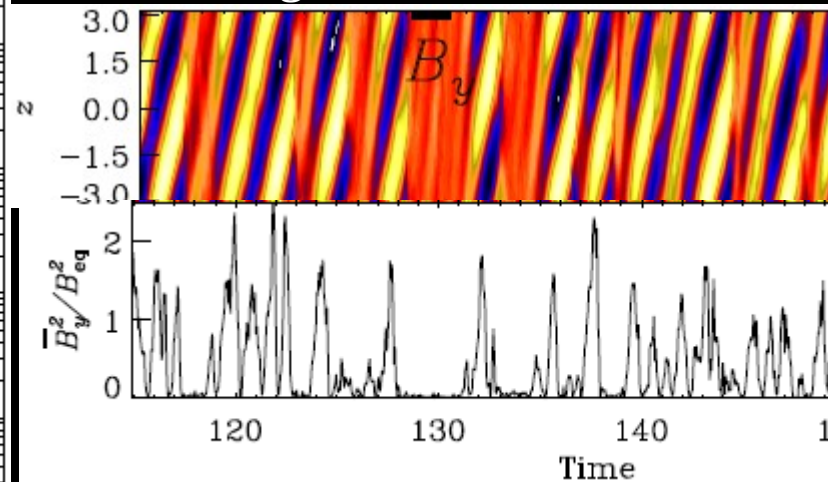
Also see Beaudoin et al. (2013)

BTW, please don't forget to come to see my poster:

**QUENCHING AND ANISOTROPY OF
HYDROMAGNETIC TURBULENT TRANSPORT
&
HYSTERESIS BETWEEN DISTINCT MODES OF
TURBULENT DYNAMOS**

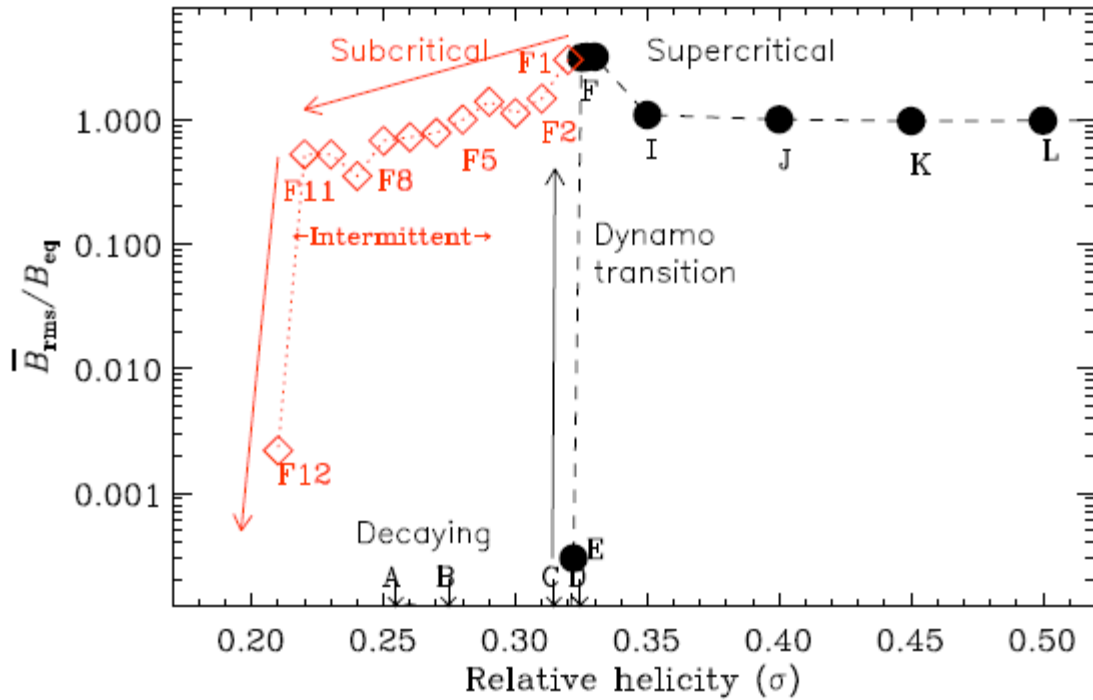


Brandenburg & Matthias Rheinhardt

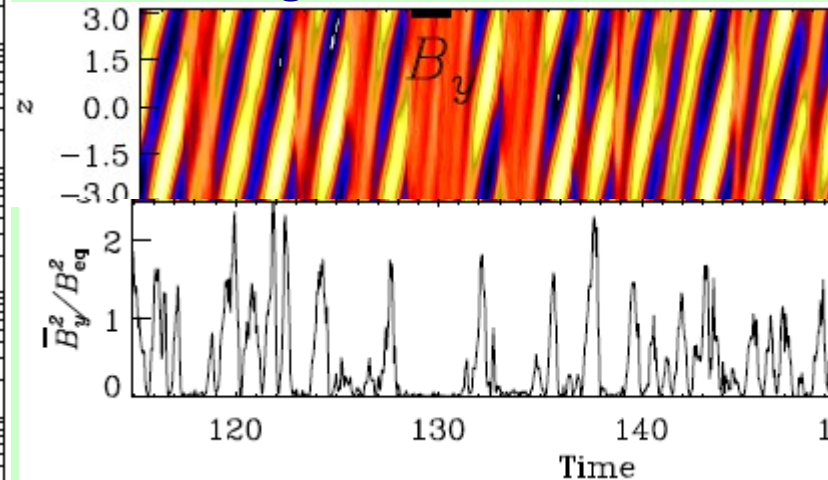


BTW, please don't forget to come to see my poster:

**QUENCHING AND ANISOTROPY OF
HYDROMAGNETIC TURBULENT TRANSPORT
&
HYSTERESIS BETWEEN DISTINCT MODES OF
TURBULENT DYNAMOS**



Brandenburg & Matthias Rheinhardt



Drivers of the meridional circulation

(Ruediger 1989; Kitchatinov & Ruediger 1995; Miesch & Hindman 2011)

$$\mathcal{D}(\psi) = \sin \vartheta r \frac{\partial \Omega^2}{\partial z} - \frac{g}{c_p r} \frac{\partial S}{\partial \vartheta} + \mathcal{G}$$

$$\mathcal{D}(\psi) = -(\mathbf{e}_\phi)_n \varepsilon_{nmi} \frac{\partial}{\partial r_m} \left(\frac{1}{\rho} \frac{\partial}{\partial r_j} \rho \mathcal{N}_{ijkl} \frac{\partial V_k^m}{\partial r_l} \right)$$

$$\mathcal{G} = \left\{ \nabla \times \left[\overline{(\nabla \times \mathbf{v}') \times \mathbf{v}'} + (4\pi\rho)^{-1} \overline{(\nabla \times \mathbf{B}) \times \mathbf{B}} \right] \right\} \cdot \hat{\phi}$$

$$\text{Ta} = (2\Omega_0 \Delta r^2 / \nu)^2, \quad (8)$$

where $\Delta r = r_1 - r_0$ is the thickness of the convecting shell. The fluid, magnetic, and SGS Prandtl numbers are defined as

$$\text{Pr} = \frac{\nu}{\chi_m}, \quad \text{Pm} = \frac{\nu}{\eta}, \quad \text{Pr}_{\text{SGS}} = \frac{\nu}{\bar{\chi}_{\text{SGS}}}, \quad (9)$$

respectively, where $\chi_m = K(r_m)/c_p \rho_m$ is the thermal diffusivity and ρ_m is the density, both evaluated at $r = r_m$. Furthermore, we define the non-dimensional viscosity,

$$\tilde{\nu} = \frac{\nu}{\sqrt{GM_\odot R_\odot}}, \quad (10)$$

and the Rayleigh and convective Rossby numbers (Gilman 1977)

$$\text{Ra} = \frac{GM_\odot (\Delta r)^4}{\nu \bar{\chi}_{\text{SGS}} R_\odot^2} \left(-\frac{1}{c_p} \frac{ds}{dr} \right)_{r_m}, \quad \text{Ro}_c = \left(\frac{\text{Ra}}{\text{Pr}_{\text{SGS}} \text{Ta}} \right)^{1/2}, \quad (11)$$

where the entropy gradient of the non-convecting hydrostatic solution is evaluated in the middle of the convection zone, $r = r_m$. We also quote the initial density contrast $\Gamma_\rho^{(0)} \equiv \rho(r_0)/\rho(r_1)$.

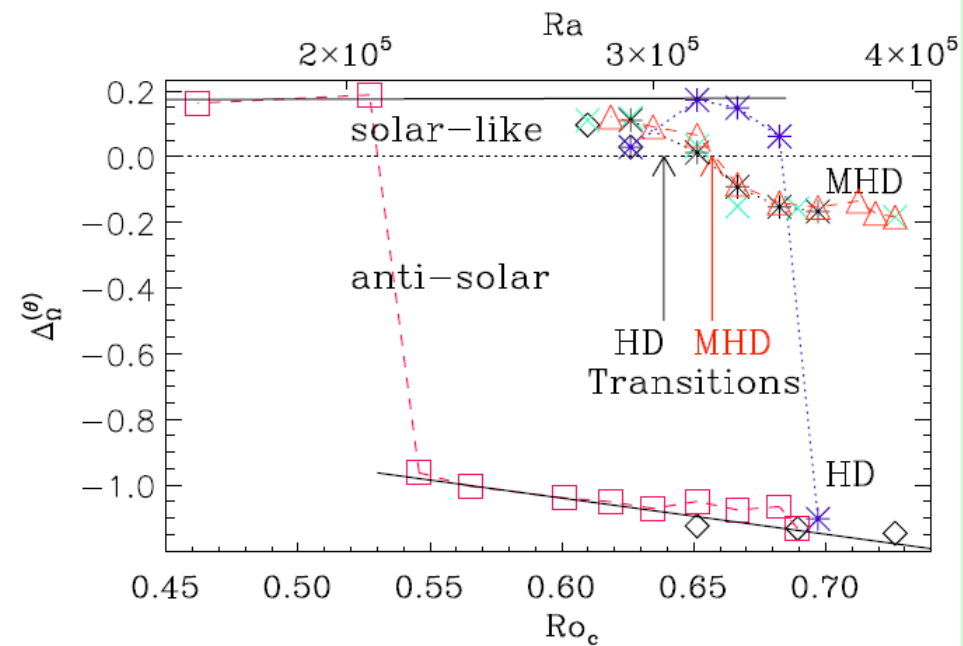
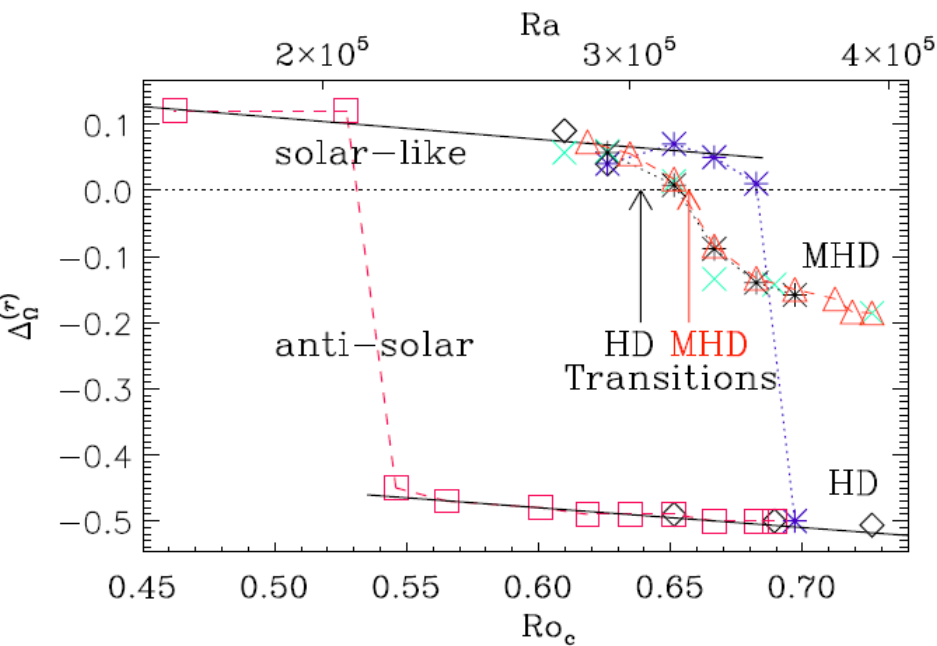
As diagnostic quantities we define the fluid and magnetic Reynolds numbers, and the Coriolis number as

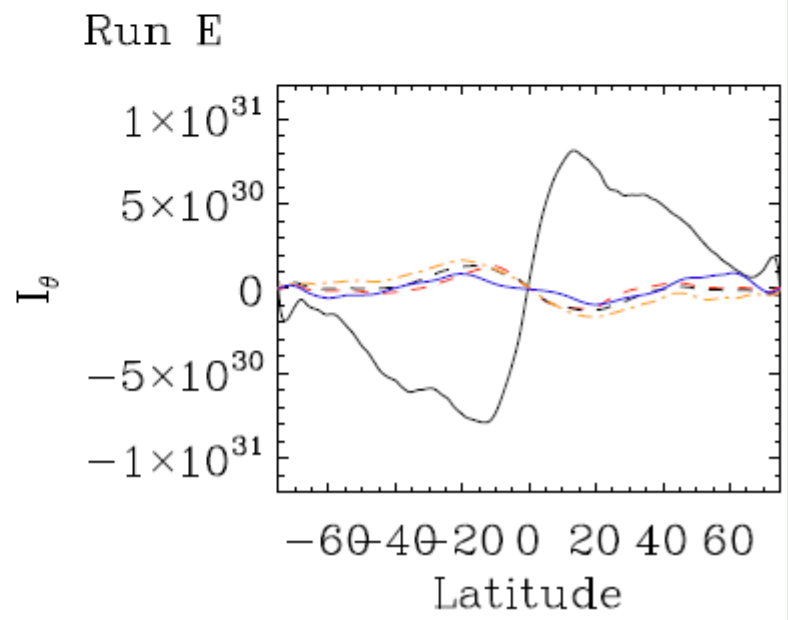
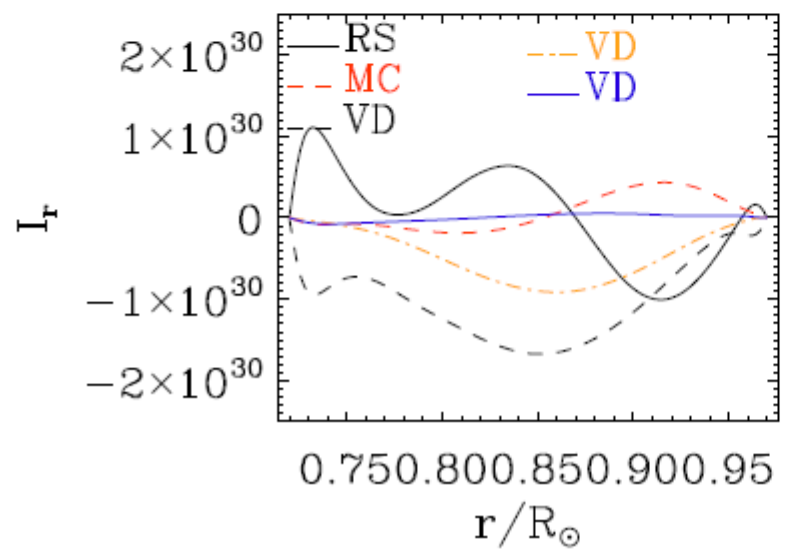
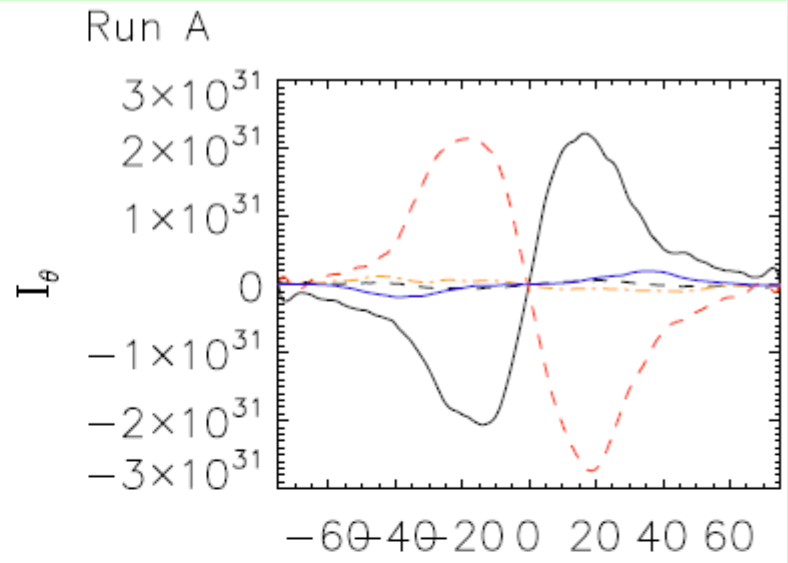
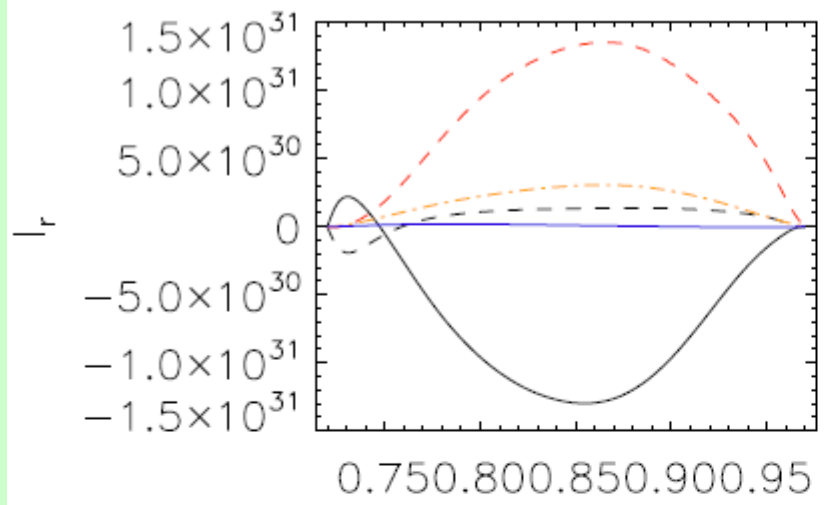
$$\text{Re} = \frac{u_{\text{rms}}}{\nu k_f}, \quad \text{Rm} = \frac{u_{\text{rms}}}{\eta k_f} = \text{PmRe}, \quad \text{Co} = \frac{2\Omega_0}{u_{\text{rms}} k_f}, \quad (12)$$

Identifying the transition of differential rotation

$$\Delta_{\Omega}^{(r)} = \frac{\Omega_{\text{eq}} - \Omega_{\text{bot}}}{\Omega_{\text{eq}}}, \quad \Delta_{\Omega}^{(\theta)} = \frac{\Omega_{\text{eq}} - \Omega_{55}}{\Omega_{\text{eq}}}, \quad (13)$$

where $\Omega_{\text{eq}} = \bar{\Omega}(r_1, \pi/2)$ and $\Omega_{\text{bot}} = \bar{\Omega}(r_0, \pi/2)$ are the equatorial rotation rates at the surface and at the base of the convection zone, and $\Omega_{55} = \frac{1}{2}[\bar{\Omega}(r_1, 35^\circ) + \bar{\Omega}(r_1, 145^\circ)]$ is the rotation rate at latitudes $\pm 55^\circ$ computed as an aver-





Boundary conditions

For velocity field: Radial and latitudinal boundaries are impenetrable and stress-free

For magnetic field: Perfect conductor at latitudinal boundaries and lower radial boundary. Radial field condition at the outer boundary

On the latitudinal boundaries we assume that the density and entropy have vanishing first derivatives.

On the upper radial boundary we apply a black body condition:

$$\sigma T^4 = -K \nabla_r T - \chi_{\text{SGS}} \rho T \nabla_r s.$$

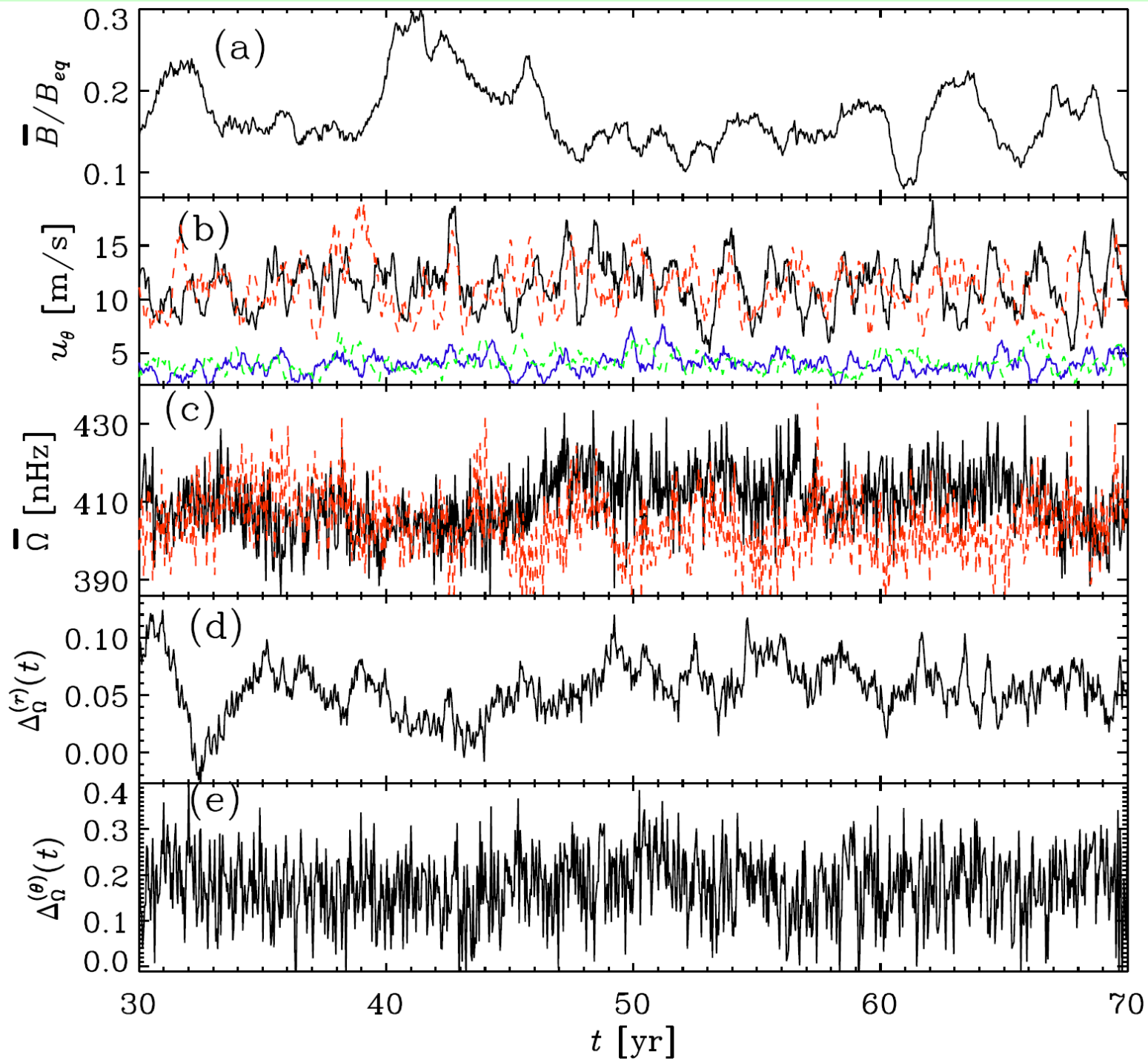
$$F_b = -\left(K \partial T / \partial r\right)_{r=r_0}$$

Initial state
isoentropic

$$\frac{\partial T}{\partial r} = -\frac{GM_{\odot}/r^2}{c_V(\gamma - 1)(n_{\text{ad}} + 1)}$$

We add a small-scale low amplitude Gaussian noise as **initial condition** for velocity and magnetic field

Run	Ra	Pr	δn	Ro _c	Re	Co	$\Delta_{\Omega}^{(\theta)}$	$\Delta_{\Omega}^{(r)}$	$\tilde{E}_{\text{kin}}[10^{-7}]$	$E_{\text{mer}}/E_{\text{kin}}$	$E_{\text{rot}}/E_{\text{kin}}$	\tilde{L}_{rad}	\tilde{L}_{conv}	DR	magnetic cycle
A	$3.93 \cdot 10^5$	39.9	2.5	0.73	33	1.34	-0.184	-0.185	0.25	3.77×10^{-3}	0.173	0.09	0.95	AS	regular
B	$3.54 \cdot 10^5$	20.3	2.25	0.69	32	1.35	-0.158	-0.143	0.24	2.87×10^{-3}	0.134	0.19	0.84	AS	regular
BC	$3.54 \cdot 10^5$	15.6	2.1	0.67	32	1.38	-0.151	-0.134	0.23	2.69×10^{-3}	0.155	0.24	0.77	AS	regular
C	$3.16 \cdot 10^5$	13.6	2.0	0.65	30	1.44	0.033	0.014	0.27	1.05×10^{-3}	0.341	0.28	0.70	SL	intermittent
D	$2.92 \cdot 10^5$	11.3	1.85	0.63	26	1.67	0.118	0.059	0.26	0.67×10^{-3}	0.487	0.33	0.57	SL	irregular
E	$2.77 \cdot 10^5$	10.2	1.75	0.61	25	1.75	0.111	0.057	0.23	0.81×10^{-3}	0.468	0.37	0.52	SL	irregular
D0	$2.92 \cdot 10^5$	11.3	1.85	0.63	26	1.67	0.118	0.059	0.26	0.67×10^{-3}	0.487	0.33	0.57	SL	irregular
D1	$3.16 \cdot 10^5$	13.6	2.00	0.65	30	1.46	0.013	0.008	0.29	1.53×10^{-3}	0.333	0.28	0.71	SL	irregular
D2	$3.31 \cdot 10^5$	15.7	2.10	0.67	31	1.40	-0.069	-0.074	0.21	1.70×10^{-3}	0.121	0.24	0.76	AS	irregular
D3	$3.47 \cdot 10^5$	18.5	2.20	0.68	32	1.38	-0.153	-0.140	0.23	2.69×10^{-3}	0.143	0.20	0.81	AS	regular
D4	$3.62 \cdot 10^5$	22.5	2.30	0.70	32	1.36	-0.167	-0.158	0.24	3.17×10^{-3}	0.149	0.17	0.86	AS	regular
A0	$3.93 \cdot 10^5$	39.9	2.5	0.73	33	1.34	-0.184	-0.185	0.25	3.77×10^{-3}	0.173	0.09	0.95	AS	regular
A1	$3.85 \cdot 10^5$	33.3	2.45	0.72	32	1.36	-0.172	-0.184	0.25	3.57×10^{-3}	0.163	0.11	0.92	AS	regular
A2	$3.78 \cdot 10^5$	28.5	2.4	0.71	32	1.36	-0.135	-0.144	0.23	2.93×10^{-3}	0.122	0.13	0.89	AS	irregular
A3	$3.62 \cdot 10^5$	22.3	2.3	0.70	32	1.38	-0.154	-0.150	0.23	2.95×10^{-3}	0.126	0.17	0.85	AS	irregular
A4	$3.47 \cdot 10^5$	18.3	2.2	0.68	32	1.38	-0.141	-0.133	0.23	2.79×10^{-3}	0.124	0.20	0.81	AS	irregular
A5	$3.31 \cdot 10^5$	15.5	2.1	0.67	31	1.41	-0.075	-0.073	0.23	2.04×10^{-3}	0.142	0.24	0.76	AS	irregular
A6	$3.16 \cdot 10^5$	13.4	2.0	0.65	30	1.44	0.066	0.017	0.24	1.40×10^{-3}	0.212	0.28	0.71	SL	irregular
A7	$3.00 \cdot 10^5$	11.9	1.9	0.63	29	1.53	0.091	0.055	0.31	0.58×10^{-3}	0.499	0.31	0.62	SL	irregular
A8	$2.85 \cdot 10^5$	10.7	1.8	0.62	27	1.61	0.121	0.073	0.29	0.61×10^{-3}	0.553	0.35	0.54	SL	irregular
B'	$3.54 \cdot 10^5$	20.3	2.25	0.69	32	1.34	-0.154	-0.149	0.21	3.66×10^{-3}	0.117	0.19	0.82	AS	regular
B''	$3.54 \cdot 10^5$	20.3	2.25	0.69	32	1.36	-0.132	-0.140	0.25	2.66×10^{-3}	0.128	0.19	0.85	AS	regular



From
Run E
(SL
Diff Rot)

Variation:
~ 40%

~ 4%

~ 50%

~ 60%